Ternary Phases (Heusler) in the System Ti-Co-Sn

ANDREY KOSINSKIY, OLE BJØRN KARLSEN, MAGNUS H. SØRBY, and ØYSTEIN PRYTZ

Some of the Heusler-phases (XY_2Z and XYZ) are known to have large homogeneity ranges which can be useful for tuning material properties. In this work, we have revised the isothermal section of the Ti-Co-Sn system at 973 K (700 °C). A total of 29 ternary compositions, mostly in the regions $TiCo_{2-x}Sn$ for $0 \leq x \leq 1$ and $Ti_{1+y}Co_2Sn_{1-y}$ for $0 \leq y \leq 1$, were prepared by arc-melting, then ball-milled and annealed. The resulting annealed powder samples were studied by applying the Rietveld method to X-ray and neutron powder diffraction data. Half-Heusler $TiCoSn$ was not observed. The Heusler phase observed in $TiCo_{2-x}Sn$ has compositions ranging from $TiCo_{1.52}Sn$ to $TiCo_2Sn$ and has the half-Heusler structure where the excess of Co is located on the semi-filled tetrahedral site $4d$ (¾, ¾, ¾) in the space group F-$43m$. At 1273 K (1000 °C), this solid solubility is expanded from $TiCo_2Sn$ to $TiCo$ with full solid solubility where Ti is gradually replacing Sn ($Ti_{1+y}Co_2Sn_{1-y}$ for $0 \leq y \leq 1$), while at 973 K (700 °C) there is a small solubility gap for $0.0 \leq y \leq 0.2$.

I. INTRODUCTION

HEUSLER-PHASES have lately received much attention in the literature, both in fundamental research and in application-focused research areas like thermoelectrics and spin-tronics.[1] Heusler compounds are divided into full-Heusler (fH) and half-Heusler (hH). Both structures are cubic where fH is described with space group Fm-$3m$ (no. 225, MnCu$_2$Al-prototype), often referred to as XY_2Z, and hH is described with space group F-$43m$ (no. 216, MgAgAs-prototype), often referred to as XYZ, where X and Y are typically transition metals and Z is a main group element.

Early works on the Ti-Co-Sn system indicated the existence of both the fH $TiCo_2Sn$ and the hH $TiCoSn$.[2,3] These works reported a solid solution $TiCo_{2-x}Sn$ that follows Vegard's law only for $x > 0.4$, while below 0.4 the lattice constant of the Heusler-phase stays very close to 6.00 Å. Later studies using extended X-ray absorption fine structure and neutron diffraction show that samples with composition $TiCoSn$ after annealing at 1073 K (800 °C) are multi-phase, where the Heusler-phase has the composition $TiCo_{1.5}Sn$ and a unit cell close to 6.00 Å.[4,5] However, the most recent studies on the Ti-Co-Sn system again report the existence of hH $TiCoSn$ with full solid solubility between hH and fH[6] or a partial solubility.[7]

This experimental work deals with annealed powder samples of ternary alloys containing Heusler-phases with elements Ti, Co and Sn. Samples were analyzed mainly by X-ray (XRD) and neutron powder diffraction (ND). The Rietveld method was used to analyze the diffraction data with respect to the compositions and unit cell parameters for the phases as well as the relative phase fractions. Based on these techniques, a revised isothermal section at 973 K (700 °C) with the focus on the Heusler-region of the phase diagram Ti-Co-Sn is proposed.

II. EXPERIMENTAL METHODS

The investigated samples were made by arc melting of elements with purity 99.9 wt pct or better. Arc melting was done in Ti-gettered argon atmosphere in a water-cooled copper hearth and a tungsten electrode. The samples were turned and re-melted 3 times to improve homogeneity. Resulting buttons of about 5 g were ball-milled in argon atmosphere for 6 minutes in a SPEX SamplePrep 8000D Mixer/Mill in chromium steel vials (SPEX 8001) with 10 chromium steel balls (14 pct Cr) of 4 g each. Sample loss in this whole synthesis process was below 1 pct of the initial weight. No contamination of the samples with iron or chromium was detected with EDS in SEM.

The powder samples were annealed in evacuated silica ampoules at the temperatures 973 K and 1273 K (700 °C and 1000 °C) followed by quenching in water. Samples #16–19 (Table I) were annealed for 21 days at 973 K (700 °C) while the rest of the samples were annealed for 7 days. Annealing at 1273 K (1000 °C) was done for 48 hours, and if no severe sample loss (described in the next paragraph) was observed, they were annealed for another 48 hours.

We chose to focus on the annealing temperature of 973 K (700 °C) since annealing at both lower and higher

ANDREY KOSINSKIY, Engineer, OLE BJØRN KARLSEN, Senior Engineer, and ØYSTEIN PRYTZ, Associate Professor, are with the Department of Physics, University of Oslo, Blindern, P.O. Box 1048, Oslo, Norway. Contact e-mail: oystein.prytz@fys.uio.no MAGNUS H. SØRBY, Senior Scientist, is with the Physics Department, Institute for Energy Technology, P.O. Box 40, Kjeller, Norway.

Table I. Equilibrium Phase Assembly in the Investigated Samples After Annealing at 973 K (700 °C)

#	Nominal Composition Ti-Co-Sn (At. Pct)	Equilibrated Phases	Phase Composition (Rietveld)	Relative Phase Amount (Mol. Pct)	Lattice Constant (s) (Å)
1	33.3-33.3-33.3**	$Ti_{1+y}Co_{2-x}Sn_{1-y}$	$TiCo_{1.52(2)}Sn$	70.4(5)	$a = 5.9994(2)$
		o-Ti_6Sn_5	—	22.1(5)	$a = 5.7047(1)$
					$b = 91116(1)$
					$c = 16.9224(3)$
		Liquid (Sn-rich)*	—	7.5(3)	$a = 5.8326(3)$
					$c = 3.1848(2)$
2	30.8-38.4-30.8	$Ti_{1+y}Co_{2-x}Sn_{1-y}$	$TiCo_{1.54(2)}Sn$	90.2(5)	$a = 5.9996(2)$
		o-Ti_6Sn_5	—	5.8(3)	$a = 5.6999(1)$
					$b = 9.1056(2)$
					$c = 16.898(4)$
		Liquid (Sn-rich)*	—	4.0(3)	$a = 5.8330(3)$
					$c = 3.1852(3)$
3	30.3-39.4-30.3	$Ti_{1+y}Co_{2-x}Sn_{1-y}$	$TiCo_{1.54(2)}Sn$	93.5(5)	$a = 5.9994(2)$
		o-Ti_6Sn_5	—	3.1(3)	$a = 5.7127(8)$
					$b = 9.115(1)$
					$c = 16.952(3)$
		Liquid (Sn-rich)*	—	3.4(3)	$a = 5.8327(3)$
					$c = 3.1842(3)$
4	29.9-40.2-29.9	$Ti_{1+y}Co_{2-x}Sn_{1-y}$	$TiCo_{1.55(1)}Sn$	96.9(5)	$a = 5.9995(1)$
		Liquid (Sn-rich)*	—	3.1(5)	$a = 5.8327(4)$
					$c = 3.1844(3)$
5	29.4-41.2-29.4	$Ti_{1+y}Co_{2-x}Sn_{1-y}$	$TiCo_{1.60(1)}Sn$	96.7(5)	$a = 6.0076(1)$
		Liquid (Sn-rich)*	—	3.3(5)	$a = 5.8329(3)$
					$c = 3.1842(3)$
6	29.0-42.0.29.0	$Ti_{1+y}Co_{2-x}Sn_{1-y}$	$TiCo_{1.65(1)}Sn$	96.5(5)	$a = 6.0181(1)$
		Liquid (Sn-rich)*	—	3.5(5)	$a = 5.8328(3)$
					$c = 3.1842(2)$
7	28.6-42.8-28.6**	$Ti_{1+y}Co_{2-x}Sn_{1-y}$	$TiCo_{1.70(1)}Sn$	97.0(5)	$a = 6.0268(1)$
		Liquid (Sn-rich)*	—	3.0(5)	$a = 5.8338(3)$
					$c = 3.1846(2)$
8	27.4-45.2-27.4	$Ti_{1+y}Co_{2-x}Sn_{1-y}$	$TiCo_{1.88(1)}Sn$	96.9(5)	$a = 6.0536(1)$
		Liquid (Sn-rich)*	—	3.1(5)	$a = 5.8335(7)$
					$c = 3.1839(6)$
9	26.6-46.7-26.6	$Ti_{1+y}Co_{2-x}Sn_{1-y}$	$TiCo_{1.92(1)}Sn$	97.9(5)	$a = 6.0674(1)$
		Liquid (Sn-rich)*	—	2.1(5)	$a = 5.8334(9)$
					$c = 3.1836(7)$
10	26.0-48.0-26.0	$Ti_{1+y}Co_{2-x}Sn_{1-y}$	$TiCo_{1.94(1)}Sn$	97.2(4)	$a = 6.0712(1)$
		CoSn	—	2.8(4)	$a = 5.2786(5)$
					$c = 4.2701(9)$
11	25.6-48.8-25.6	$Ti_{1+y}Co_{2-x}Sn_{1-y}$	$TiCo_{1.98(2)}Sn$	96.7(5)	$a = 6.0769(2)$
		CoSn	—	3.3(5)	$a = 5.2801(4)$
					$c = 4.2659(8)$
12	25.3-49.4-25.3	$Ti_{1+y}Co_{2-x}Sn_{1-y}$	$TiCo_{2.00(2)}Sn$	97.3(4)	$a = 6.0799(3)$
		CoSn	—	2.7(4)	$a = 5.279(1)$
					$c = 4.264(1)$
13	25.0-50.0-25.0**	$Ti_{1+y}Co_{2-x}Sn_{1-y}$	$TiCo_{2.00(2)}Sn_{0.97(2)}$	96.4(5)	$a = 6.0795(2)$
		Co_3Sn_2	—	3.6(5)	$a = 4.1126(5)$
					$c = 5.1864(8)$
14	24.4-51.2-24.4	$Ti_{1+y}Co_{2-x}Sn_{1-y}$	$TiCo_{2.00(2)}Sn_{0.96(2)}$	97.4(4)	$a = 6.0790(1)$
		Co_3Sn_2	—	2.6(4)	$a = 4.106(1)$
					$c = 5.199(3)$
15	23.8-52.4-23.8	$Ti_{1+y}Co_{2-x}Sn_{1-y}$	$TiCo_{2.00(2)}Sn_{0.97(2)}$	96.0(5)	$a = 6.0788(1)$
		Co_3Sn_2	—	1.7(5)	$a = 4.097(2)$
					$c = 5.197(4)$
		Co	—	2.3(5)	$a = 3.5485(9)$
16	27.5-50.0-22.5	$Ti_{1+y}Co_{2-x}Sn_{1-y}$	$Ti_{1.05(3)}Co_2Sn_{0.95(3)}$	39.4(4)	$a = 6.0820(3)$
		$Ti_{1+y}Co_{2-x}Sn_{1-y}$	$Ti_{1.28(3)}Co_2Sn_{0.72(3)}$	59.4(3)	$a = 6.0732(4)$
		Co_3Ti	—	1.2(2)	$a = 3.620(6)$

Table I.   continued

#	Nominal Composition Ti-Co-Sn (At. Pct)	Equilibrated Phases	Phase Composition (Rietveld)	Relative Phase Amount (Mol. Pct)	Lattice Constant (s) (Å)
17	30.0-50.0-20.0	$Ti_{1+y}Co_{2-x}Sn_{1-y}$	$Ti_{1.23(1)}Co_2Sn_{0.77(1)}$	97.4(2)	$a = 6.0677(5)$
		Co_3Ti	—	1.3(2)	$a = 3.6202(3)$
		$c\text{-}Co_2Ti/h\text{-}Co_2Ti^†$	—	1.3(3)	$a = 6.710(3)/$
					$a = 4.747(3)$
					$c = 15.52(2)$
18	32.5-50.0-17.5	$Ti_{1+y}Co_{2-x}Sn_{1-y}$	$Ti_{1.32(1)}Co_2Sn_{0.68(1)}$	96.9(2)	$a = 6.06058(4)$
		$c\text{-}Co_2Ti$	—	3.1(2)	$a = 6.7116(8)$
19	35.0-50.0-15.0	$Ti_{1+y}Co_{2-x}Sn_{1-y}$	$Ti_{1.45(2)}Co_2Sn_{0.55(2)}$	98.8(3)	$a = 6.04752(5)$
		$c\text{-}Co_2Ti$	—	1.2(3)	$a = 6.721(4)$
20	40.0-50.0-10.0	$Ti_{1+y}Co_{2-x}Sn_{1-y}$	$Ti_{1.70(2)}Co_2Sn_{0.30(2)}$	99.4(2)	$a = 6.03206(5)$
		$c\text{-}Co_2Ti$	—	0.6(2)	$a = 6.727(5)$
21	70.0-10.0-20.0‡	$Ti_{1+y}Co_{2-x}Sn_{1-y}$	$Ti_{1.95(3)}Co_2Sn_{0.05(3)}$	—	$a = 5.993(1)$
		$CoTi_2$	—	—	$a = 11.303(1)$
		Ti_3Sn	—	—	$a = 5.9156(3)$
					$c = 4.7609(4)$
22	45.0-45.0-10.0	$Ti_{1+y}Co_{2-x}Sn_{1-y}$	$Ti_{1.79(3)}Co_2Sn_{0.21(3)}$	89.0(7)	$a = 6.02410(6)$
		$Ti_5Sn_3Co_{1-x}$	Ti_5Sn_3Co	11.0(7)	$a = 8.1122(7)$
					$c = 5.5308(8)$
23	40.0-52.0-8.0	$Ti_{1+y}Co_{2-x}Sn_{1-y}$	$Ti_{1.75(2)}Co_2Sn_{0.25(2)}$	93.1(8)	$a = 6.02488(7)$
		$c\text{-}Co_2Ti$	—	6.9(8)	$a = 6.7152(5)$
24	40.0-40.0-20.0	$Ti_{1+y}Co_{2-x}Sn_{1-y}$	$Ti_{1.36(3)}Co_2Sn_{0.64(3)}$	76.7(3)	$a = 6.03812(2)$
		$Ti_5Sn_3Co_{1-x}$	Ti_5Sn_3Co	23.2(3)	$a = 8.1310(2)$
					$c = 5.5424(2)$
25	35.0-55.0-10.0	$Ti_{1+y}Co_{2-x}Sn_{1-y}$	$Ti_{1.58(1)}Co_2Sn_{0.42(1)}$	81.2(4)	$a = 6.02794(5)$
		$c\text{-}Co_2Ti$	—	18.8(4)	$a = 6.7146(2)$
26	30.0-60.0-10.0	$Ti_{1+y}Co_{2-x}Sn_{1-y}$	$Ti_{1.27(2)}Co_{1.95(3)}Sn_{0.73(2)}$	53.9(3)	$a = 6.0580(1)$
		Co_3Ti	—	26.5(2)	$a = 3.6205(4)$
		$h\text{-}Co_2Ti$	—	19.6(2)	$a = 4.747(1)$
					$c = 15.486(6)$
27	35.0-35.0-30.0	$TiCo_{2-x}Sn$	$TiCo_{1.57(3)}Sn$	72.7(2)	$a = 5.99874(3)$
		$o\text{-}Ti_6Sn_5$	—	27.3(2)	$a = 5.7142(2)$
					$b = 9.1206(4)$
					$c = 16.9489(7)$
28	30.0-45.0-25.0	$Ti_{1+y}Co_{2-x}Sn_{1-y}$	$Ti_{1.16(2)}Co_{1.74(2)}Sn_{0.84(2)}$	100	$a = 6.03625(5)$
29	25.0-55.0-20.0	$Ti_{1+y}Co_{2-x}Sn_{1-y}$	$Ti_{1.16(2)}Co_2Sn_{0.84(2)}$	87.4(2)	$a = 6.07887(5)$
		Co_3Ti	—	1.5(2)	$a = 3.6126(6)$
		Co	—	11.1(2)	$a = 3.5570(1)$

Obtained by Rietveld refinement of XRD data. Numbers in parentheses show standard deviations derived from the Rietveld refinements.
*Liquid solidifies mostly as β-Sn during quenching. Relative phase amount and unit cell parameters are given for this phase.
**These samples were analyzed both with XRD and ND.
†Difficult to determine which of the two Co_2Ti phases (cubic or hexagonal) that is present.
‡Difficult to quantify relative phase amounts by XRD because $Ti_{1.95(3)}Co_2Sn_{0.05(3)}$ is ductile.
— compositions are not refined for these phases.

temperatures for some of these compositions is problematic. At temperatures 873 K (600 °C) and lower, most of the powder samples are not homogenized after annealing for 1 month. When annealed at temperatures above 1073 K (800 °C), samples that contain the phase Ti_6Sn_5 are found to form an oxide layer on the walls of the silica glass ampoule. The area of the ampoule wall that is in direct contact with the sample becomes coated with a Ti-Sn-oxide, while the rest of the ampoule becomes fully coated with an amorphous Ti-oxide of about 1 μm in thickness. Carbon coating of the ampoule wall does not hinder this process, but it can be suppressed by reducing the inner area of the ampoule, i.e., by soldering a silica rod just above the sample inside the ampoule. The amount of these oxides is relatively low compared to the amount of sample (<1 wt pct), but it involves only two of the components in the sample.

Powder X-ray diffraction (XRD) was done with a Bruker AXS D8 Discover in Bragg-Brentano geometry with Ge(111)-monochromated Cu Kα$_1$-radiation and LynxEye™ 1D strip detector with energy filtering to suppress the Co-fluorescence. Data were collected on glass plate holders in the 2θ range of 20 to 120 deg with step-size 0.015 deg. Silicon standard NIST 640d with the lattice constant $a = 5.43123$ Å was used as internal standard for the XRD measurements. Some samples were also analyzed with ND for a different scattering contrast between the elements as compared to X-rays (neutron scattering lengths: $b_{Ti} = -3.4$, $b_{Co} = 2.5$, $b_{Sn} = 6.2$ fm). ND experiments were done at the JEEP II research reactor facility at Kjeller in Norway, on the
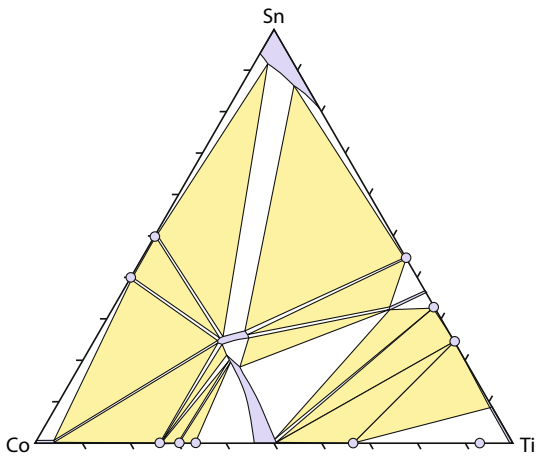
Fig. 1—The proposed isothermal section at 973 K (700 °C) of the ternary phase diagram Ti-Co-Sn. The single phase regions are colored in blue and three-phase regions in yellow to facilitate reading. (At 1273 K (1000 °C) the solubility gap between two solubility regions around $Ti_{25}Co_{50}Sn_{25}$ disappears).

diffractometer PUS equipped with a focusing composite Ge monochromator and two detector banks with 7 ^{3}He-filled position-sensitive detector tubes in each. The sample was contained in a vanadium sample holder with 6 mm inner diameter. Data were collected in the 2θ range 10 to 130 deg with a wavelength of 1.5548 Å for samples $Ti_{33.3}Co_{33.3}Sn_{33.3}$ and $Ti_{28.6}Co_{42.8}Sn_{28.6}$ and 1.5539 Å for the sample $Ti_{25.0}Co_{50.0}Sn_{25.0}$. Rietveld analysis was carried out with the software Bruker's Topas[8] for XRD and GSAS EXPGUI+[9,10] for ND.

Standard deviations derived from the Rietveld refinements are given in parentheses after the refined values.

III. EXPERIMENTAL RESULTS AND DISCUSSION

Twenty-nine different compositions within the Ti-Co-Sn system have been investigated in this work and the samples annealed at 973 K (700 °C) are summarized in Table I. Space groups of the phases used in Rietveld refinements are listed in Table II.

We propose a revised isothermal section at 973 K (700 °C) (Figure 1) based on the observed phase relations that are listed in Table I.

A solid solubility range (SSR) $TiCo_{2-x}Sn$ ($x \leq 0.48$) was observed in the investigated temperature interval 973 K to 1273 K (700 °C to 1000 °C); however, no hH with composition TiCoSn was found.

The SSR $TiCo_{2-x}Sn$ has space group F-43m with Wyckoff-positions $4a$ (0, 0, 0), $4b$ (½, ½, ½) and $4c$ (¼, ¼, ¼), fully occupied with Ti, Sn and Co; respectively, while the excess Co is located in the Wyckoff-position $4d$ (¾, ¾, ¾) with site occupancy between 0.52 and 1.0 (Figure 2). A Co $4d$ occupancy of 0.52 gives composition $TiCo_{1.52}Sn$ while occupancy 1.0 gives composition $TiCo_2Sn$. Rietveld refinement of the diffraction data clearly show that at larger values of x (lower amount of Co) the hH structure describes the observed SSR better than the fH-structure, but at values of x around 0.3 (higher Co-content) these two models become indistinguishable. After all, the composition $TiCo_2Sn$ is a fH where the Wyckoff-position $8c$ in the

Table II. The Space Group of the Observed Phases

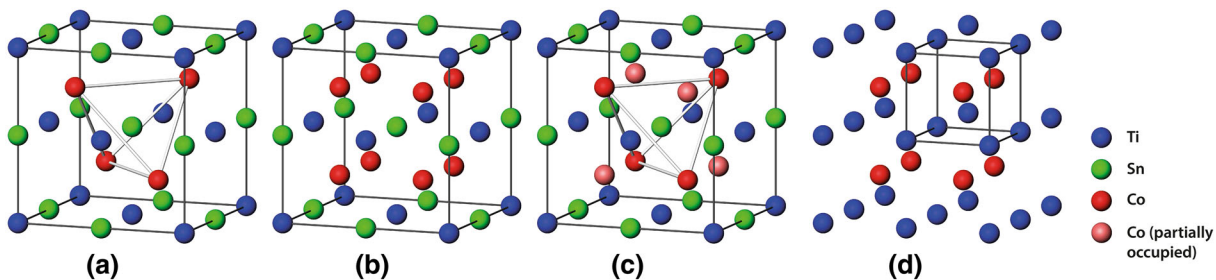| Compound	Space Group	Compound	Space Group
$Ti_{1+y}Co_{2-x}Sn_{1-y}$	F-43m	$CoTi_2$	Fd-3m
$Ti_5Sn_3Co_{1-x}$[11]	$P6_3/mcm$	Ti_3Sn	$P6_3/mmc$
Co	Fm-3m	o-Ti_6Sn_5	$Immm$
Co_3Ti	Pm-3m	β-Sn	$I4_1/amd$
c-Co_2Ti	Fd-3m	CoSn	P6/mmm
h-Co_2Ti	$P6_3/mmc$	Co_3Sn_2	$P6_3/mmc$

Fig. 2—The unit cell of (a) half-Heusler (hH) (F-43m), (b) full-Heusler (fH) (Fm-3m), (c) proposed intermediate-Heusler (iH) (F-43m) and (d) TiCo (Pm-3m). For all of the Heusler structures Ti is in $4a$ (0, 0, 0); for hH, fH and iH Sn is in $4b$ (½, ½, ½); for hH Co is in $4c$ (¼, ¼, ¼) while $4d$ (¾, ¾, ¾) is unoccupied, while for iH $4d$ (¾, ¾, ¾) is partially occupied; for fH Co is in $8c$ (¼, ¼, ¼). For TiCo Ti is in $1a$ (0,0,0) and Co is in $1b$ (½, ½, ½).

Table III. Refinement Results from XRD of the iH-Phase in Samples with Composition Ti$_{25.0}$Co$_{50.0}$Sn$_{25.0}$ After Different Annealing Temperatures

Annealing Temperature [K (°C)]	a (Å)	Occupation of the Element on its Wyckoff Position		
		4a (Ti)	4b (Sn)	4c + 4d (Co)
773 (500)	6.0707 (2)	1.00	0.95 (2)	1.97 (2)
973 (700)	6.0795 (2)	1.00	0.97 (2)	2.00 (2)
1273 (1000)	6.0721 (2)	1.00	1.00 (2)	2.00 (2)

Position 4a is locked to full occupation by Ti in the refinement as a normalizing parameter.

space group *Fm-3m* is fully occupied by Co, which is equivalent to having fully occupied Wyckoff-positions 4c and 4d in the space group *F-43m*. For convenience, we chose to call this SSR intermediate Heusler (iH) (Figure 2).

Samples with composition Ti$_{33.3}$Co$_{33.3}$Sn$_{33.3}$ contain three phases after annealing at 973 K (700 °C). XRD and ND show that the iH-phase is the main phase in these samples and has composition TiCo$_{1.52(2)}$Sn and a = 5.9994(2) Å (Table I). After annealing at 1273 K (1000 °C), the sample consists of iH-phase with phase composition TiCo$_{1.60(2)}$Sn and a = 6.0139(2) Å (70.7 wt pct), Ti$_6$Sn$_5$ (rt) (4.8 wt pct) and Sn-rich liquid that is solidified dominantly into the phase β-Sn (24.5 wt pct) during quenching. (On the diffraction pattern of 1273 K (1000 °C) some additional weak reflections are present that cannot be indexed to known intermetallic phases of Ti, Co and Sn.) These iH-phase compositions make one of the end points of the SSR TiCo$_{2-x}$Sn, and from these observations we can see that the temperature dependence of x goes as follows: $x \leq 0.48$ for 973 K (700 °C) and $x \leq 0.40$ for 1273 K (1000 °C).

Anti-site disorder between Co and Ti in the Ti$_{25.0}$Co$_{50.0}$Sn$_{25.0}$ (fH composition) has previously been studied by ^{119}Sn Mössbauer spectroscopy and ^{59}Co nuclear magnetic resonance spectroscopy.[12] The reported distortion of a local probe of a sample annealed at 800 K (527 °C) for 14 days is (Ti$_{0.91}$Co$_{0.09}$)(Co$_{1.91}$Ti$_{0.09}$)Sn with a = 6.0718(3) Å (from XRD). Our observations from XRD show a similar lattice constant a = 6.0707(1) Å in a sample with nominal composition Ti$_{25.0}$Co$_{50.0}$Sn$_{25.0}$ annealed at 773 K (500 °C), but no anti-site disorder between Co and Ti is observed. Instead, the Rietveld refinement shows that the site of Sn (4b) is missing 5 pct scattering intensity in XRD, which might indicate vacancies or a small substitution of the lighter elements Co or Ti on the Sn site. Samples annealed at 973 K (700 °C) have a larger lattice constant a = 6.0797(1) Å and show no indication of disorder. These values are supported by ND experiments. However, samples annealed at 1273 K (1000 °C) have a lower lattice constant a = 6.0721(2) Å for the iH-phase and show no indication of any large disorder in the structure (Table III).

It should be emphasized that the samples in the compositional range between Ti$_{33.3}$Co$_{33.3}$Sn$_{33.3}$ and Ti$_{25.0}$Co$_{50.0}$Sn$_{25.0}$ are not single phase. They consist of the iH-phase together with secondary phases (Table I). From the relative amounts of phases obtained by Rietveld refinements, without taking any substitutions mechanisms into account, the composition of the iH can be calculated. This shows that the composition of the iH is enriched in Ti and Co. This effect is largest for Ti and gives 0.7 at. pct excess Ti in the iH for sample Ti$_{25.0}$Co$_{50.0}$Sn$_{25.0}$ and 3 at. pct for Ti$_{33.3}$Co$_{33.3}$Sn$_{33.3}$. One explanation for this could be that the excess of the Ti atoms is allocated on the semi-filled 4d site (¾, ¾, ¾), something that will be hard to establish by Rietveld refinement of XRD data since the scattering difference of Co and Ti is so small that XRD is unreliable. For the compositions close to fH, the 4d site fills up and in sample Ti$_{25.0}$Co$_{50.0}$Sn$_{25.0}$ there is no room for allowing Ti in 4d (¾, ¾, ¾). From the refinement, we see that sites 4a, 4c and 4d are fully occupied with, respectively, Ti and Co at 973 K (700 °C) (Table III). However, 4b, the Sn position, has a scattering deficiency of 3 pct. Vacancies on the Sn site would be in accordance with the observation, but so also would be substitution of Ti/Co for Sn. Later, we will show that for TiCo$_2$Sn substitution of Ti for Sn indeed takes place.

Similar off-stoichiometry has been reported in the closely related system, Ti-Ni-Sn. Samples of TiCo$_2$Sn show similar off-stoichiometry where the reported fH has the composition Ti$_{23.3}$Ni$_{52.2}$Sn$_{24.4}$ after annealing at 1223 K (950 °C). The authors explained this as Ti/Ni substitution on the Sn site 4b.[13] Off-stoichiometry is also reported for the annealed samples TiNiSn containing mostly hH, but phases Ti$_6$Sn$_5$ and β-Sn are also present.[14]

Samples with compositions Ti$_{33.3}$Co$_{33.3}$Sn$_{33.3}$, Ti$_{28.6}$Co$_{42.8}$Sn$_{28.6}$ and Ti$_{25.0}$Co$_{50.0}$Sn$_{25.0}$, all annealed at 973 K (700 °C) (Table I; Figure 3), were analyzed with ND. All of these samples give small diffraction peaks at d = 2.44(1) and 1.27(1) Å that fit to a cubic cell with a = 4.23(1) Å, possibly related to a divalent oxide of Ti or/and Co. These peaks were not observed in the XRD patterns. This can possibly be attributed to the specimen size where the amount of analyzed sample for the XRD is in the order of milligrams while the amount of the sample for ND is in the order of grams. In the refinement, the peaks were modeled as TiO (*Fm-3m*) and were found to make up about 0.5(2) wt pct.

In this work, we have also discovered a previously unreported SSR between the compositions Ti$_{25.0}$Co$_{50.0}$Sn$_{25.0}$ and Ti$_{50.0}$Co$_{50.0}$ (Table IV). At 1273 K (1000 °C), there is full solubility of Ti on the Sn-site (0.0 ≤ y ≤ 1.0), but at 973 K (700 °C) there is a solubility gap that
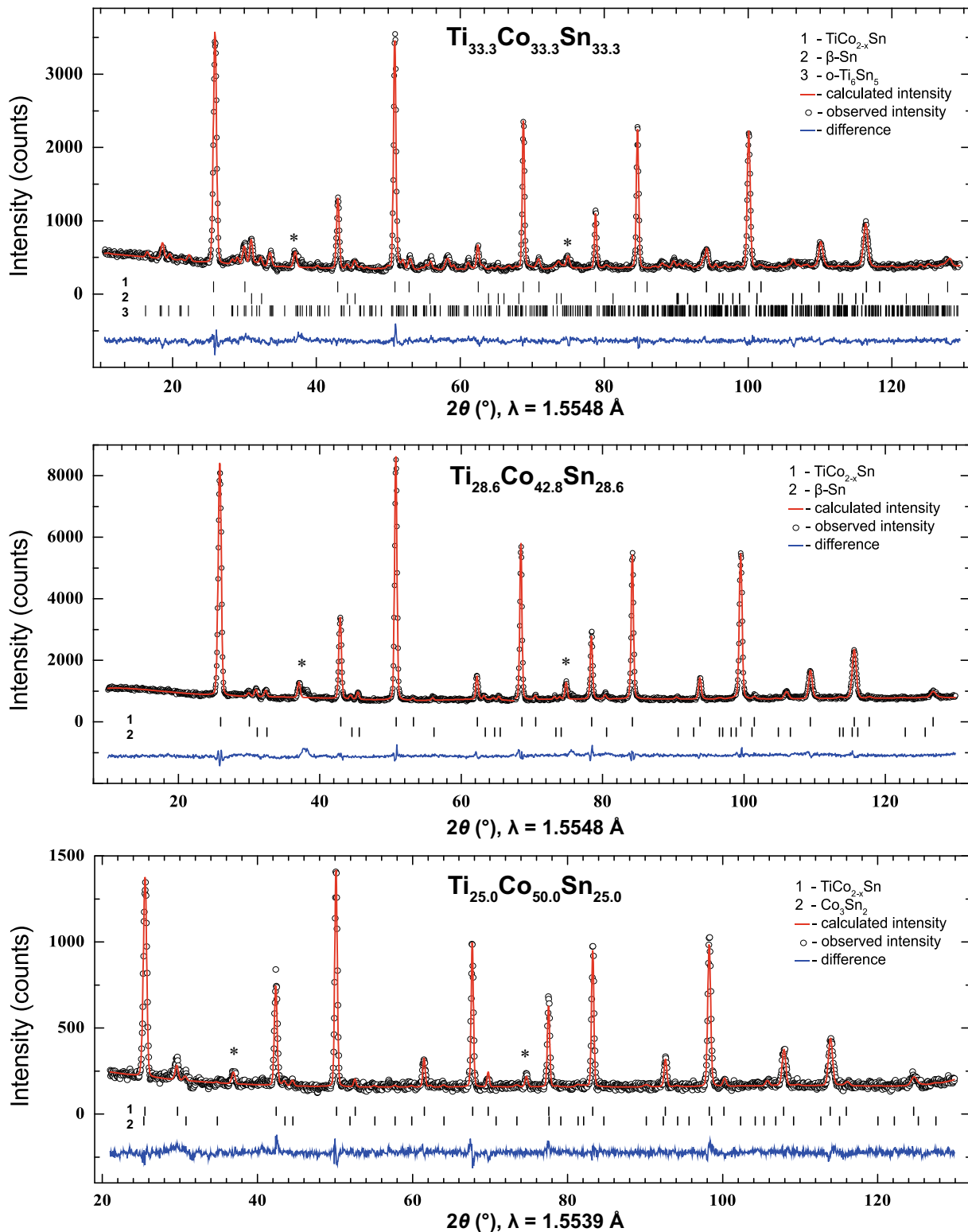
Fig. 3—ND data from samples $Ti_{33.3}Co_{33.3}Sn_{33.3}$, $Ti_{28.6}Co_{42.8}Sn_{28.6}$ and $Ti_{25.0}Co_{50.0}Sn_{25.0}$ after annealing at 973 K (700 °C). Peaks marked with (*) were modeled as TiO with a = 4.23 (1) Å (see text).

reduces the solubility range to $0.2 \leq y \leq 1.0$. Together with the SSR $TiCo_{2-x}Sn$, they form a larger solid solution $Ti_{1+y}Co_{2-x}Sn_{1-y}$ (Figures 1 and 4).

A similarly large solubility region at 1123 K (850 °C) has recently been found in the system Ti-Ni-Sn that extends between $TiNi-TiNi_2Sn-TiNi_{1.654}Sn$.[13] In this

Table IV. Refinement Results from XRD of the Heusler-Phase in Selected Samples Within Composition Range $Ti_{1+y}Co_2Sn_{1-y}$ After Annealing at 973 K and 1273 K (700 °C and 1000 °C)

| | Heusler-Phase in the Samples | | | |
| | 973 K (700 °C) Annealing | | 1273 K (1000 °C) Annealing | |
Sample Composition	a (Å)	Phase Composition	a (Å)	Phase Composition
$Ti_{25.0}Co_{50.0}Sn_{25.0}$	6.0795 (2)	$TiCo_2Sn_{0.97(2)}$	6.0721 (2)	$Ti_{1.00(1)}Co_{1.99(1)}Sn_{1.00(1)}$
$Ti_{27.5}Co_{50.0}Sn_{22.5}$	6.0820 (3)	$Ti_{1.05(3)}Co_2Sn_{0.95(3)}$	6.06780 (3)	$Ti_{1.14(2)}Co_{2.00(1)}Sn_{0.86(2)}$
	6.0732 (4)	$Ti_{1.28(3)}Co_2Sn_{0.72(3)}$		
$Ti_{30.0}Co_{50.0}Sn_{20.0}$	6.0677 (5)	$Ti_{1.23(1)}Co_2Sn_{0.77(1)}$	6.05992 (4)	$Ti_{1.21(2)}Co_{1.95(2)}Sn_{0.79(2)}$
$Ti_{32.5}Co_{50.0}Sn_{17.5}$	6.06058 (4)	$Ti_{1.32(1)}Co_2Sn_{0.68(1)}$	6.05117 (3)	$Ti_{1.29(2)}Co_{2.00(1)}Sn_{0.71(2)}$
$Ti_{35.0}Co_{50.0}Sn_{15.0}$	6.04752 (5)	$Ti_{1.45(2)}Co_2Sn_{0.55(2)}$	6.04323 (3)	$Ti_{1.40(1)}Co_{1.96(1)}Sn_{0.60(1)}$

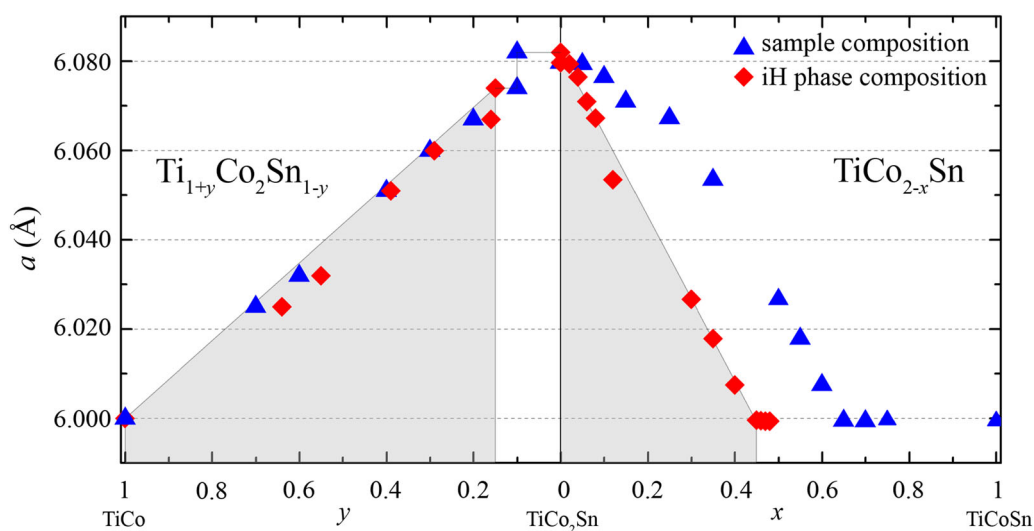Values for 973 K (700 °C) are taken from Table I.

Fig. 4—Compositional dependence of the lattice parameters for solid solubility regions $Ti_{1+y}Co_2Sn_{1-y}$ and $TiCo_{2-x}Sn$ in the samples annealed at 973 K (700 °C) (from Table I). Blue triangles mark the nominal composition of the sample and red diamonds mark the refined iH-phase composition for that sample (sample with $y = 0.1$ contains two iH phases). Homogeneity regions are shaded. The deviation between sample and iH composition is due to the presence of other phases, see text. The value of a for $y = 1$ is taken from Ref. [15].

system, there is a small solubility gap between $Ti_{1.68}Ni_2Sn_{0.32}$ and $Ti_{1.64}Ni_2Sn_{0.34}$.

There is full solid solubility ($Ti_{1+y}Co_2Sn_{1-y}$ for $0 \leq y \leq 1.0$) in the samples within this compositional range after annealing at 1273 K (1000 °C). However, samples annealed at 973 K (700 °C) indicate a solubility gap in the composition range $0.0 \leq x \leq 0.2$. This manifests itself as shoulders on the iH-peaks in the XRD data (Figure 5). The shape of this shoulder remains the same even after increased annealing time up to 1 month at 973 K (700 °C). After annealing at 1273 K (1000 °C), the diffraction data of these samples are easily fitted with one Heusler-like phase with sharp peaks. Re-annealing down from 1273 K (1000 °C)

makes the peaks broader, which indicates phase separation, and shifts the a-axis back to larger values. Since the shoulder reappears after re-annealing, there are grounds to assume that compositions with $0.0 \leq y \leq 0.2$ experience a transition from a single-phase to a two-phase area somewhere between 973 K and 1273 K (700 °C and 1000 °C). Surprisingly, the lattice constants a for the iH-phases within this SSR become noticeably lower with the increase in the annealing temperature; for instance, $Ti_{35.0}Co_{50.0}Sn_{15.0}$ contains iH-phase with $a = 6.04752(5)$ Å after annealing at 973 K (700 °C) and 6.04323(3) Å after annealing at 1273 K (1000 °C) (Table IV and Figure 5).
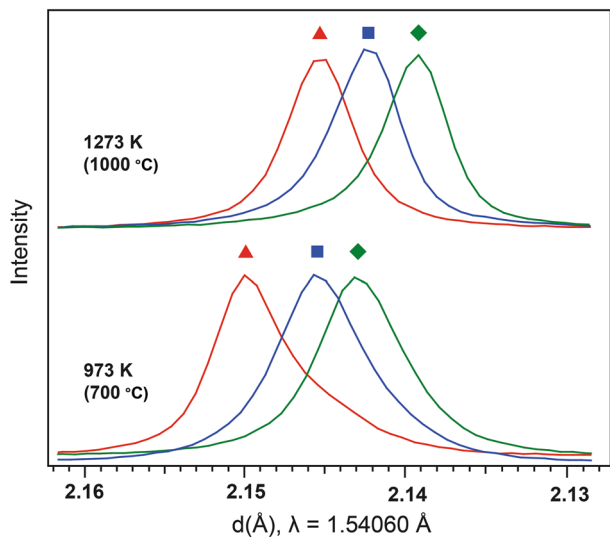
Fig. 5—220-peaks of the iH phases in samples $Ti_{27.5}Co_{50.0}Sn_{22.5}$ (red triangle), $Ti_{30.0}Co_{50.0}Sn_{20.0}$ (blue square) and $Ti_{32.5}Co_{50.0}Sn_{17.5}$ (green diamond) after annealing at 973 K and 1273 K (700 °C and 1000 °C). A distinctive shoulder is visible for the $Ti_{27.5}Co_{50.0}Sn_{22.5}$ annealed at 973 K (700 °C).

These two solid solubility ranges form together a continuous solid solution at 1273 K (1000 °C) that may be written schematically as $Ti_{1+y}Co_{2-x}Sn_{1-y}$ for ($0 \leq x \leq 0.40$ and $y = 0$; or $0 \leq y \leq 1$ and $x = 0$), while at 973 K (700 °C) there is a gap in the composition and thus the solid solution can be written as ($0 \leq x \leq 0.48$ and $y = 0$; or $0.2 \leq y \leq 1$ and $x = 0$) (Figure 4). This fact that none of the samples on the compositional line $TiCo_2Sn$-$TiCoSn$ are single phase at 973 K (700 °C) complicates the representation of the figure.

IV. CONCLUSIONS

In this work, we have revised the isothermal section at 973 K (700 °C) of the ternary system Ti-Co-Sn. The main focus of the study was to explore the phase relationships around the Heusler-phases. The stoichiometric half-Heusler TiCoSn was not found to be present. Solid solution from $TiCo_2Sn$ to $TiCo_{1.52}Sn$ at 973 K (700 °C) has been established. In addition, a solid solution between $TiCo_2Sn$ and TiCo, with Ti substitution for Sn, has been shown to exist. This solid solution

is full at 1273 K (1000 °C) but has a miscibility gap at 973 K (700 °C). The full solubility range of the Heusler-related phases may be written as $0 \leq x \leq 0.48$ and $y = 0$; or $0.2 \leq y \leq 1$ and $x = 0$ at 973 K (700 °C) and $0 \leq x \leq 0.40$ and $y = 0$; or $0 \leq y \leq 1$ and $x = 0$ at 1273 K (1000 °C).

REFERENCES

1. T. Graf, C. Felser, and S.S.P. Parkin: *Prog. Solid State Chem.*, 2011, vol. 39, p. 1.
2. J. Pierre, R.V. Skolozdra, and Yu.V. Stadnyk: *J. Magn. Magn. Mater.*, 1993, vol. 128, p. 93.
3. R.V. Skolozdra, Yu.V. Stadnyk, Yu.K. Gorelenko, and E.E. Terletkaya: *Sov. Phys. Solid State*, 1990, vol. 32, p. 1536.
4. T. Nobata, G. Nakamoto, M. Kurisu, Y. Makihara, T. Tokuyoshi, and I. Nakai: *Jpn. J. Appl. Phys.*, 1999, vol. 38, p. 429.
5. T. Nobata, G. Nakamoto, M. Kurisu, Y. Makihara, K. Ohoyama, and M. Ohashi: *J. Alloys Compd.*, 2002, vol. 347, p. 86.
6. Yu. Stadnyk, L. Romaka, A. Horyn, A. Tkachuk, Yu. Gorelenko, and P. Rogl: *J. Alloys Compd*, 2005, vol. 387, p. 251.
7. C. Colinet, J.-C. Tedenac, and S.G. Fries: *CALPHAD*, 2009, vol. 33, p. 250.
8. A.A. Coelho: *Bruker AXS*, Karlsruhe, Germany, 2006.
9. A.C. Larson and R.B. Von Dreele: Los Alamos National Laboratory Report LAUR, 2000, p. 86.
10. B.H. Toby: *J. Appl. Cryst.*, 2001, vol. 34, p. 210.
11. J.C. Schuster, M. Naka, and T. Shibayanagi: *J. Alloys Compd.*, 2000, vol. 305, p. L1.
12. H.C. Kandpal, V. Ksenofontov, M. Wojcik, R. Seshadri, and C. Felser: *J. Phys. D*, 2007, vol. 40, p. 1587.
13. M. Gürth, A. Grytsiv, J. Vrestal, V.V. Romaka, G. Giester, E. Bauer, and P. Rogl: *RSC Advances*, 2015, vol. 5, p. 92270.
14. J.E. Douglas, C.S. Birkel, N. Verma, V.M. Miller, M.-S. Miao, G.D. Stucky, T.M. Pollock, and R. Seshadri: *J. Appl. Phys.*, 2014, vol. 115, p. 043720.
15. T. Takasugi and O. Izumi: *Phys. Status Solidi A*, 1987, vol. 102, p. 697.